

M/C-TH 00/08
HD-THEP-00-50
October 2000

Diffractive Exclusive Photon Production in Deep Inelastic Scattering

A Donnachie

Department of Physics and Astronomy, University of Manchester,
Manchester, M13 9PL, England¹

and

H G Dosch

Institut für Theoretische Physik der Universität Heidelberg
Philosophenweg 16, 69120 Heidelberg, Germany

and

The Erwin Schrödinger Institute for Mathematical Physics
Boltzmannngasse 9, A-1090 Wien, Austria

Abstract

Predictions for Deep Virtual Compton Scattering are obtained in a two component dipole model of diffraction. The model automatically includes hard and soft components and implicitly allows for “hadronic” contributions via large dipoles. It is also applicable to real Compton Scattering, which provides an important constraint.

¹email: ad@theory.ph.man.ac.uk; h.g.dosch@thphys.uni-heidelberg.de

1 Introduction

Deep Virtual Compton Scattering (DVCS) on protons, $\gamma^*p \rightarrow \gamma p$, is an important reaction for the study of diffraction. In the standard perturbative QCD approach the amplitude is described by skewed parton distributions [1] for $Q^2 > Q_0^2$, for some non-zero Q_0^2 . The skewed parton distributions correspond to operator products evaluated between protons of unequal momenta. These are generalisations of the familiar parton distributions of deep inelastic scattering, and like them satisfy perturbative evolution equations [2] which enable them to be evaluated at all Q^2 in terms of an assumed input at some appropriate $Q^2 = Q_0^2$.

Preliminary data have been presented [3] which are consistent with QCD predictions [4]. The QCD calculations require the input skewed parton distributions at the reference point Q_0^2 . In [4] these are obtained by estimating their ratio to “ordinary” parton distributions at $Q_0^2 = 2.5 \text{ GeV}^2$ using arguments based on the aligned jet model [5]. In practice this is equivalent [6] to the simplest diagonal generalised vector meson dominance model [7]. The rôle of vector mesons, particularly the ρ , in providing a “hadronic” contribution to DVCS via the vector-meson-dominance mechanism $\gamma^*p \rightarrow Vp, V \rightarrow \gamma$ has been calculated in [6] and shown to be important at values of Q^2 well beyond the input reference point Q_0^2 .

The model of ρ electroproduction used in [6] is a two-component model, combining soft and hard contributions which are respectively primarily non-perturbative and perturbative in origin. There is considerable evidence in γ^*p interactions that the nominally perturbative regime can be strongly influenced by non-perturbative effects. This is an obvious feature of dipole models of deep inelastic scattering [8]–[14], where the contribution from large dipoles can extend to significantly large values of Q^2 ; and in two-component models [15]–[19], in which there is a non-perturbative term at all Q^2 by construction.

Here we present the results of a model which incorporates these effects not in the language of parton distributions but rather that of dipole cross sections. In the framework of functional integration a two-component dipole cross section is constructed based on the approach of [16, 18]. The model covers the complete range from the real γp cross section through DVCS, with one photon virtual, to deep inelastic scattering, with both photons virtual. The model as applied to DVCS contains no free parameters at $t = t_{\min}$: they have already been determined from the pp and γ^*p total cross sections. To obtain the integrated cross section requires knowledge of the logarithmic slope of the differential cross section. This can also be determined from the model, and for ρ electroproduction [20] is in good agreement with the experimental value over the relevant range of Q^2 . We use this as a reasonable estimate in the present dipole approach.

2 The model

We present a calculation for the cross section of Compton scattering with different virtualities of the photons. The treatment is based on a functional approach of high energy scattering with small momentum transfer [21] in which the scattering of a $q\bar{q}$ pair is expressed as the functional average of a Wegner-Wilson loop with light-like sides [22, 23]. The functional average is performed in a model for non-perturbative QCD [24, 25]. The model depends essentially on two typically non-perturbative parameters: the strength of the gluon correlator, given through the gluon condensate $\langle g^2 FF \rangle$, and its correlation length a . The linear confining potential is also defined in terms of these two parameters [24, 25]. Nucleons are most simply treated as a quark-diquark system, that is effectively as a dipole, although this is not essential. The two parameters of the model were obtained by fitting the isoscalar part of $\bar{p}p$ and pp scattering at $W = 20$ GeV, and were found to be $\langle g^2 FF \rangle = 2.49$ GeV⁴ and $a = 0.346$ fm. These values are within the range determined from lattice calculations, and give the correct value for the slope of the confining potential.

In this approach scattering amplitudes with small momentum transfer can also be calculated, but in this note we concentrate on forward scattering. Then the approach becomes a simple dipole model and the Compton scattering amplitude can be expressed as an integral over the product of the dipole-proton cross section $\sigma_d(R)$ and the overlap of the photon wave functions with virtualities Q_1^2 and Q_2^2 and helicity λ , $\rho_\gamma^\lambda(Q_1^2, Q_2^2, R, z)$:

$$T(s, t = 0) = 2\pi \int_0^1 dz \int dR R \rho_\gamma^\lambda(Q_1^2, Q_2^2, R, z) \sigma_d(R) \quad (1)$$

where z is the longitudinal momentum fraction of the quark in the photons and R is the radius of the quark-antiquark dipole, the weak dependence of the dipole cross section [20] is neglected. The dipole cross section $\sigma_d(R)$ as evaluated in the model can be very well described by

$$\sigma_d(R) = 0.098 \left(\langle g^2 FF \rangle a^4 \right)^2 R \left(1 - \exp \left(- \frac{R}{3.1a} \right) \right) \quad (2)$$

The dimensionless constant $\langle g^2 FF \rangle a^4$ has the numerical value 23.8. If a and R are measured in fermi, the result is in millibarn.

As it stands the model has no energy dependence. The increase with energy of hadronic cross sections as $W^{2\epsilon_{\text{soft}}}$, where the intercept of the pomeron trajectory is $1 + \epsilon_{\text{soft}}$ with $\epsilon_{\text{soft}} \sim 0.09 \pm 0.01$, can be incorporated in two ways. Either one lets the radii of hadrons increase with W^2 [23],[26]–[28], or one takes the model as a determination of the coefficient of pomeron exchange and includes a factor $(W/W_0)^{2\epsilon_{\text{soft}}}$ with $W_0 = 20$ GeV. These two approaches give very similar results and we adopt the latter in this paper as it is the more convenient in the present context.

To incorporate the greater energy dependence observed in reactions with a hard scale, such as deep inelastic scattering, the two-pomeron approach of [15] was adapted to the model in [16] and applied successfully to the photo- and electro-production of vector mesons and to the proton structure function over a wide range of Q^2 . As in [15] it was found that the soft-pomeron contribution to the proton structure function initially increases with increasing Q^2 , has a broad maximum in the region of 5 GeV² and then decreases slowly as Q^2 decreases further. In the context of the present model this is a consequence of the decreasing interaction strength with decreasing dipole size.

It is worth recalling the salient features of this version of the two-pomeron model to illustrate the distinction between the soft- and hard-pomeron contributions. Following [16] it is assumed that all dipole amplitudes in which both dipoles are larger than the correlation length $a = 0.346$ fm are dominated by the soft pomeron, and the energy dependence is given by $(W/W_0)^{2\epsilon_{\text{soft}}}$. This ensures that the hard pomeron has essentially no impact on purely hadronic scattering. If at least one of the dipoles is smaller than a fm then the energy dependence is replaced by $(W/W_0)^{2\epsilon_{\text{hard}}}$, with $\epsilon_{\text{hard}} = 0.42$. This is the value found by [15] and is larger than the value used in [16]. This difference in $\epsilon_{\text{hard}} = 0.42$ between the present paper and [16] is accounted for by a different treatment of the z integration. In [16] there was a cutoff in the z integration, requiring that $Wz(1-z) > 0.2$ GeV in order to ensure that the quarks in the centre-of-mass frame have at least this energy. This z cutoff introduces an additional energy dependence, particularly for highly virtual photons. In our approach we follow the general lines of the dipole models and integrate z from zero to one and therefore need a higher intercept for the hard component. It was found in [16] that the extrapolation of the non-perturbative model to high values of Q^2 overestimates the small dipole contributions and therefore the dipole cross section is put to zero below a radius $R_c = 0.16$ fm.

The quark-antiquark overlap density of photons with virtuality Q_1^2 and Q_2^2 respectively and helicity λ in lowest order perturbation theory is

$$\begin{aligned}\rho_\gamma^0(Q_1^2, Q_2^2, R, z) &= \frac{2N_c\alpha}{\pi^2} e_f^2 Q_1 Q_2 z^2 (1-z)^2 K_0(\epsilon_1 R) K_0(\epsilon_2 R) \\ \rho_\gamma^{\pm 1}(Q_1^2, Q_2^2, R, z) &= \frac{2N_c\alpha}{\pi^2} e_f^2 \left((z^2 + (1-z)^2) \epsilon_1 K_1(\epsilon_1 R) \epsilon_2 K_1(\epsilon_2 R) \right. \\ &\quad \left. + m_f^2 K_0(\epsilon_1 R) K_0(\epsilon_2 R) \right).\end{aligned}\tag{3}$$

Here e_f is the charge of the quark in units of the elementary charge; m_f is the Lagrangian quark mass; $\epsilon_i = \sqrt{z(1-z)Q_i^2 + m_f^2}$; $\lambda = 0$ indicates a longitudinal photon and $\lambda = \pm 1$ indicates a transverse photon. The singularities of the Bessel functions at $R = 0$ do not cause any problems, since for the evaluation of observable amplitudes the density is multiplied by the dipole cross section which is proportional to R^2 for small values of R .

For longitudinal photons the factor $z^2(1-z)^2$ in the density ρ_γ^λ ensures that

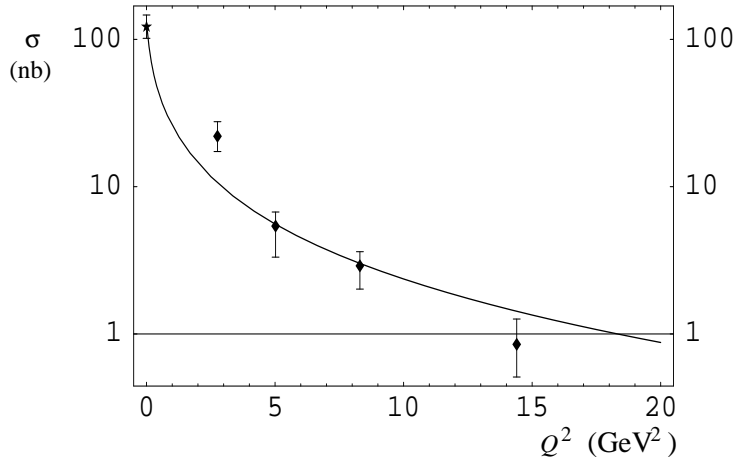


Figure 1: The integrated cross section for the reaction $\gamma^* p \rightarrow \gamma p$ as function of the virtuality Q^2 of the incoming photon at an average $\langle W \rangle = 75$ GeV

the main contribution comes from the region $z \approx \frac{1}{2}$, and the relevant scale is $\frac{1}{4}Q^2 + m_f^2$. Thus contributions from large dipoles are suppressed at large Q^2 . However for transverse photons the endpoints $z = 0$ and $z = 1$ are not suppressed and large dipoles can contribute to the perturbative regime even if the virtuality is quite high. The z cutoff of [16] mentioned above is therefore most important for large values of Q_i^2 .

The results (3) are reliable for large values of Q^2 and/or large quark masses. For small values of Q^2 and light quarks the separation of the quark-antiquark pair can become large and confinement effects become important. An effective way in which to deal with this problem is to introduce a Q^2 -dependent effective constituent quark mass as an infrared regulator in the photon wave function. This procedure is justified in [29] where the value of the light quark effective mass at $Q^2 = 0$ is determined from the two-point function of the vector current as $m_{0q} = 0.21 \pm 0.015$ GeV and for the strange quark as $m_{0s} \approx 0.31$ GeV. Since in this note we consider only processes where one photon is real we always use these effective mass values at $Q^2 = 0$. The charmed quark mass was taken as $m_c = 1.3$ GeV.

3 Results

A convenient fit to the model calculation for $0 \leq Q^2 \leq 100$ GeV² (good in the amplitudes up to 1 % for $Q^2 < 20$ GeV² and 3 % for higher Q^2 values) for one

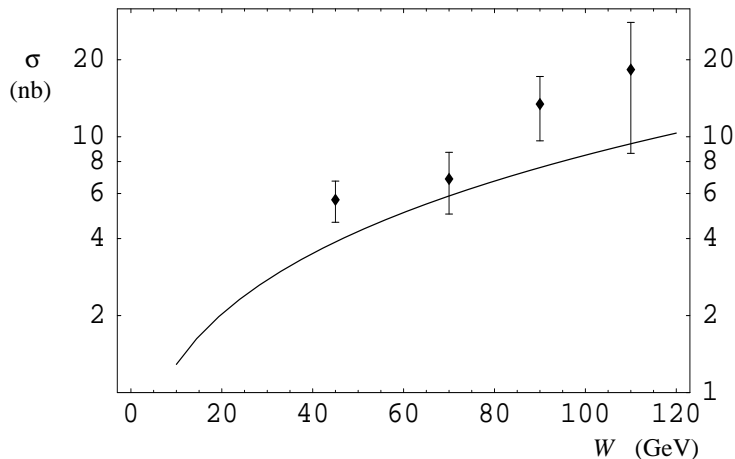


Figure 2: The integrated cross section for the reaction $\gamma^* p \rightarrow \gamma p$ as function of the center-of-mass energy W at an average virtuality of the incoming photon of $\langle Q^2 \rangle = 4.5 \text{ GeV}^2$

photon real, the other one with virtuality Q^2 is given by:

$$\frac{d\sigma}{dt}(Q^2, W, t = t_{min}) = \frac{1}{16\pi} \left(r_{\text{soft}}(Q^2) (W/W_0)^{0.16} + r_{\text{hard}}(Q^2) (W/W_0)^{0.84} \right)^2 311 \mu\text{b}/\text{GeV}^2 \quad (4)$$

where $W_0 = 20 \text{ GeV}$ and

$$\begin{aligned} r_{\text{soft}}(Q^2) &= \left(5.33 - 1.33 \exp(-4Q^2/Q_0^2) + 5.37 Q^2/Q_0^2 \right)^{-1} \\ r_{\text{hard}}(Q^2) &= \left(49.42 - 7.65 \exp(-4Q^2/Q_0^2) + 4.94 Q^2/Q_0^2 \right)^{-1} \end{aligned} \quad (5)$$

with $Q_0^2 = 1 \text{ GeV}^2$. The present calculation provides the $\gamma^* p \rightarrow \gamma p$ amplitude only for forward scattering, that is at $t = t_{min} \approx -m_{\text{proton}}^2 Q^2/s^2$, so it is necessary to make an assumption about the t -dependence to obtain an integrated cross section. As the process is dominated by light-quark dipoles, it is reasonable to take the t -dependence to be similar to that for ρ electroproduction. For definiteness we take the logarithmic slope to be $B = 7 \text{ GeV}^{-2}$, which is the average value over the Q^2 range of the preliminary H1 data [3]. Such a value of the average slope is also the result of model calculation for electroproduction of ρ mesons [20, 31].

The relation between the $ep \rightarrow ep\gamma$ cross section and the $\gamma^* p \rightarrow \gamma p$ cross section is [30]

$$\frac{d^2\sigma_{ep \rightarrow ep\gamma}}{dW dQ^2} = \frac{\alpha_{\text{em}}}{\pi} \frac{W}{Q^2(W^2 + Q^2 - m_{\text{proton}}^2)} (1 + (1-y)^2) \sigma_{\gamma^* p \rightarrow \gamma p}, \quad (6)$$

with $y \equiv (W^2 + Q^2 - m_{\text{proton}}^2)/(s - m_{\text{proton}}^2)$. Here \sqrt{s} is the centre-of-mass energy of the ep system and W is that of the γ^*p system.

The Q^2 dependence and energy dependence of the predicted integrated $\gamma^*p \rightarrow \gamma p$ cross sections are given in figures 1 and 2 respectively. The preliminary H1 data [3] are for $ep \rightarrow ep\gamma$ and contain a large background from the QED Bethe-Heitler process. However as the latter is purely real and as the QCD amplitude is mainly imaginary (the real part is expected to be only about 10 – 15% of the imaginary part), interference is not large and the Bethe-Heitler cross section can simply be subtracted. A comparison with the preliminary H1 data after subtraction of the Bethe-Heitler is made in figures 1 and 2, where we have converted the experimental $ep \rightarrow ep\gamma$ to $\gamma^*p \rightarrow \gamma p$, after subtraction of the Bethe-Heitler cross section, using (6). The only serious discrepancy between the model and the preliminary data is at $Q^2 = 3.5 \text{ GeV}^2$. This is reflected in the normalisation of the integrated cross section in figure 2 as the low- Q^2 point dominates this cross section. We simply note that the inclusion of the real γp data is seen to provide an important constraint on models.

References

- [1] D Mueller et al: Fortschr.Phys. **42** (1994) 101
A Radyushkin: Phys.Lett. **B380** (1996) 417
X Ji: Phys.Rev.Lett. **78** (1977) 610; Phys.Rev. **D55** (1997) 7114
- [2] X Ji et al: Phys.Rev. **D56** (1997) 5511
A Radyushkin: Phys.Rev. **D56** (1997) 5554
I Musatov and A Radyushkin: Phys.Rev. **D61** (2000) 074027
A Belitsky et al: Phys.Lett. **B474** (2000) 163
- [3] H1 collaboration: paper submitted to the 30th International Conference on High Energy Physics, Osaka, July 2000
- [4] L Frankfurt, A Freund and M Strikman: Phys.Rev. **D58** (1998) 114001;
erratum **D59** (1999) 119901
- [5] J D Bjorken and J B Kogut: Phys.Rev. **D8** (1973) 1341
- [6] A Donnachie, J Gravelis and G Shaw: hep-ph/0009235
- [7] J J Sakurai and D Schildknecht: Phys.Lett. **40B** (1972) 121;
Phys.Lett. **41B** (1972) 489; Phys.Lett. **42B** (1972) 216
- [8] J Nemchik, N N Nikolaev, E Predazzi and B G Zakharov: Z.Phys. **C75** (1997) 71
- [9] K Golec-Biernat and M Wusthoff: Phys.Rev **D59** (1999) 014017; Phys.Rev **D60** (1999) 114023
- [10] J R Forshaw, G Kerley and G Shaw: Phys.Rev. **D60** (1999) 074012;
Nucl.Phys. **A675** (2000) 80
- [11] W Buchmuller, T Gehrman and A Hebecker: Nucl.Phys. **B537** (1999) 477
- [12] M McDermott, L Frankfurt, V Guzey and A Hebecker: hep-ph/9912547
- [13] G R Kerley and M McDermott: J Phys. **G26** (2000) 683
- [14] L Frankfurt, M McDermott and M Strikman: hep-ph/0009086
- [15] A Donnachie and P V Landshoff: Phys.Lett. **B437** (1998) 408; Phys.Lett. **B470** (1999) 243; Phys.Lett. **B478** (2000) 146
- [16] M Rueter: Eur.Phys.J **C7** (1999) 233
- [17] J Kwiecinski and L Motyka: Phys.Lett. **B462** (1999) 203
- [18] A Donnachie, H G Dosch and M Rueter: Phys.Rev. **D58** (1999) 074011;
Eur.Phys.J **C13** (2000) 141

- [19] E Gotsman, E Levin, U Maor and E Naftali; Eur.Phys.J **C10** (1999) 689;
Eur.Phys.J **C14** (2000) 511
- [20] H G Dosch, T Gousset, G Kulzinger and H J Pirner: Phys.Rev **55** (1997)
2602
- [21] O Nachtmann: Ann.Phys. **209** (1991) 436
- [22] A Krämer and H G Dosch: Phys.Lett. **B272** (1991) 114
- [23] H G Dosch, E Ferreira and A Krämer: Phys.Rev. **D50** (1992) 1994
- [24] H G Dosch: Phys.Lett. **190B** (1987) 177
- [25] H G Dosch and Yu A Simonov: Phys.Lett. **205B** (1988) 339
- [26] E Ferreira and F Pereira: Phys.Rev. **D56** (1997) 179
- [27] E R Berger and O Nachtmann: Eur.Phys.J **C7** (1999) 459
- [28] F Perreira and E Ferreira: Phys.Rev. **D61** (2000) 077507
- [29] H G Dosch, T Gousset and H J Pirner: Phys.Rev. **D57** (1998) 1666
- [30] ZEUS collaboration, M Derrick et al: Z.Phys. **C63** (1998) 247
- [31] A Donnachie, J Gravelis and G Shaw: in preparation
- [32] J Breitweg et al, ZEUS Collaboration: Eur.Phys.J. **C2** (1999) 603
- [33] C Adloff et al, H1 Collaboration: Eur.Phys.J. **C13** (2000) 371